



## Molecular Crystals and Liquid Crystals

Publication details, including instructions for authors and subscription information:

<http://www.tandfonline.com/loi/gmcl20>

## Equivalent Circuit Models in Organic Light-Emitting Diodes Designed Using a Cole-Cole Plot

S. M. Han<sup>a</sup>, K. P. Kim<sup>a</sup>, D. C. Choo<sup>b</sup>, T. W. Kim<sup>b</sup>,  
J. H. Seo<sup>c</sup> & Y. K. Kim<sup>c</sup>

<sup>a</sup> Department of Information Display Engineering,  
Hanyang University, Seongdong-gu, Seoul, Korea

<sup>b</sup> Research Institute of Information Display, Division  
of Electronics and Computer Engineering, Hanyang  
University, Seongdong-gu, Seoul, Korea

<sup>c</sup> Department of Information Display Engineering &  
Center for Organic Materials & Information Display  
(COMID), Hong-ik University, Seoul, Korea

Version of record first published: 22 Sep 2010

To cite this article: S. M. Han, K. P. Kim, D. C. Choo, T. W. Kim, J. H. Seo & Y. K. Kim (2007): Equivalent Circuit Models in Organic Light-Emitting Diodes Designed Using a Cole-Cole Plot, *Molecular Crystals and Liquid Crystals*, 470:1, 279-287

To link to this article: <http://dx.doi.org/10.1080/15421400701495989>

PLEASE SCROLL DOWN FOR ARTICLE

Full terms and conditions of use: <http://www.tandfonline.com/page/terms-and-conditions>

This article may be used for research, teaching, and private study purposes. Any substantial or systematic reproduction, redistribution, reselling, loan,

sub-licensing, systematic supply, or distribution in any form to anyone is expressly forbidden.

The publisher does not give any warranty express or implied or make any representation that the contents will be complete or accurate or up to date. The accuracy of any instructions, formulae, and drug doses should be independently verified with primary sources. The publisher shall not be liable for any loss, actions, claims, proceedings, demand, or costs or damages whatsoever or howsoever caused arising directly or indirectly in connection with or arising out of the use of this material.

## Equivalent Circuit Models in Organic Light-Emitting Diodes Designed Using a Cole-Cole Plot

**S. M. Han**

**K. P. Kim**

Department of Information Display Engineering, Hanyang University,  
Seongdong-gu, Seoul, Korea

**D. C. Choo**

**T. W. Kim**

Research Institute of Information Display, Division of Electronics  
and Computer Engineering, Hanyang University, Seongdong-gu,  
Seoul, Korea

**J. H. Seo**

**Y. K. Kim**

Department of Information Display Engineering & Center for Organic  
Materials & Information Display (COMID), Hong-ik University, Seoul,  
Korea

*The equivalent circuit models in organic light-emitting diodes (OLEDs) consisting of indium-tin-oxide (ITO)/tris(8-hydroxyquinoline) Aluminum (Alq<sub>3</sub>)/Aluminum (Al), ITO/Alq<sub>3</sub>/Lithium quinolate/Al or ITO/N,N-bis-(1-naphthyl)-N,N'-diphenyl-1,1'-biphenyl-4,4'-diamine (NPB)/Alq<sub>3</sub>/Al were investigated. The relaxation times were obtained from the impedances as functions of frequencies, and the equivalent circuits in the OLEDs were designed by using the relaxation times of OLEDs determined from the impedance spectroscopies. The Cole-Cole plots calculated from the equivalent circuit models were in reasonable agreements with the experimental results. These results can help designing equivalent circuit models of multilayer OLEDs.*

**Keywords:** cole-cole plot; equivalent circuit model; impedance spectroscopy; organic light emitting diodes

**PACS Numbers:** 68.55.jk, 72.15.Eb, and 73.20.At

This work was supported by the Korea Research Foundation Grant funded by the Korean Government (MOEHRD, Basic Research Promotion Fund) (KRF-2006-005-J04102).

Address corresponding to T. W. Kim, Research Institute of Information Display, Division of Electronics and Computer Engineering, Hanyang University, 17 Haengdang-dong, Seoul, Seongdong-gu, 133-791, Korea. E-mail: twk@hanyang.ac.kr

## I. INTRODUCTION

Organic light-emitting diodes (OLEDs) have emerged as potential candidates for applications in full-color flat-panel displays because of their unique advantages of low driving voltage, low power consumption, high contrast, wide viewing angle, low cost, large flexibility, and fast response [1–5]. However, relatively few potential applications of OLEDs in full-color flat-panel displays have driven extensive efforts to enhance the efficiency and the color stabilization of the OLEDs [6,7]. The electrical and optical properties of the OLEDs have been the most extensively studied subjects. Works have been performed on the frequency-dependent electrical properties of the OLEDs, which describe transportation and charge injection mechanisms [8–11]. Even though some studies on the electrical impedance and capacitance of OLEDs consisting of small molecules or polymers have been performed [12–16], systematic studies concerning the modeling of equivalent circuits of OLEDs using Cole-Cole plots are necessary for designing the driving circuits of the OLEDs [17–19]. Furthermore, detailed understandings of the impedance spectroscopy of OLEDs consisting of small molecules have not been completed yet.

This article reports the equivalent circuit models in single and double layer OLEDs, deposited by using organic molecular-beam deposition (OMBD), designed using a Cole-Cole plot. The relaxation times of dipoles in OLEDs were determined from the impedances as functions of the frequencies, and the equivalent circuit models were designed using these results. The equivalent circuit model of a double layer OLED was designed using that of a single layer OLED by comparing with the relaxation times of three kinds of devices. The experimental results of the Cole-Cole plots were compared with the calculated results. The designed equivalent circuit model of the double layer OLEDs is described to utilize the circuit models of the multilayer OLEDs.

## II. EXPERIMENTAL DETAILS

Three kinds of samples were deposited on the indium tin oxide (ITO) thin films coated on glass substrates by using OMBD. The sheet resistivity of the ITO thin films coated on glass substrates used in this study was  $15 \Omega/\text{sq.}$ . The ITO coated substrates were cleaned using acetone and methanol at  $60^\circ\text{C}$  for 15 min in ultrasonic baths, and rinsed in de-ionized water thoroughly. The chemically cleaned ITO coated substrates had been dried by using  $\text{N}_2$  gas with a purity of 99.9999%, and the surface of the ITO coated substrates were treated

with an oxygen plasma for 2 min at an  $O_2$  pressure of approximately  $2 \times 10^{-2}$  Torr. The three kinds of samples used in this study were consisted of the following structures from the top: an Al (100 nm) cathode electrode, various kinds of organic layers, an ITO anode electrode, and glass substrates. The organic layers consisted of a tris-(8-hydroxyquinoline) aluminum ( $Alq_3$ ) (60 nm), a lithium quinolate (Liq) (2 nm)/ $Alq_3$ (60 nm), or an  $Alq_3$ (60 nm)/N,N-bis-(1-naphthyl)-N,N'-diphenyl-1,1'-biphenyl-4,4'-diamine (NPB) (50 nm). The organic and metal layers consisting of the three kinds of OLEDs were deposited at a substrate of room temperature and vacuum pressure of  $5 \times 10^{-6}$  Torr. The OLEDs with an  $Alq_3$  layer, a Liq/ $Alq_3$  layer, or an  $Alq_3$ /NPB layer are denoted by devices I, II, and III, respectively. Schematic diagrams of the three kinds of OLEDs of devices I, II, and III and the corresponding equivalent circuit models for OLEDs with a single or a double organic layer are shown in Figure 1(a) and 1(b), respectively.

The serial resistance ( $R_s$ ) is the contact resistances of OLEDs, and the  $R_p$  and the  $C_p$  are the parallel resistance and capacitance of the single layer in the OLEDs, respectively. The  $R_{p1}$  and  $C_{p1}$  are the parallel resistance and capacitance of one layer in the double layer, respectively, and the  $R_{p2}$  and  $C_{p2}$  are the parallel resistance and capacitance of the other layer in the double layer, respectively. The deposition rates of the organic layers and the metal layers were approximately 0.1 and 0.5 Å/s, respectively. The current density – voltage and luminance – voltage characteristics of devices I, II, and III were measured on a programmable electrometer with

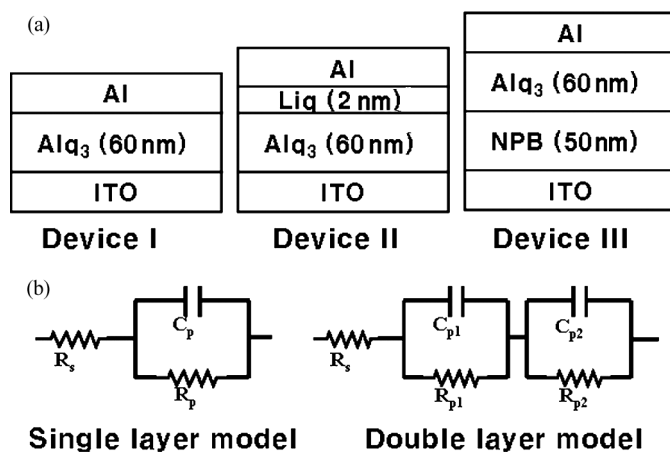


**FIGURE 1** (a) Schematic diagrams of the OLEDs of devices I, II, and III, and (b) equivalent circuit models for a single and a double layer devices.

built-in current and voltage measurement units (model 236, Keithely), and their luminance-voltage characteristics were measured by using a brightness meter (chroma meter CS-100A, Minolta). The impedance-frequency characteristics of devices I, II, and III were performed by using LCR meter (HP4284A, Hewlett Packard).

### III. RESULTS AND DISCUSSION

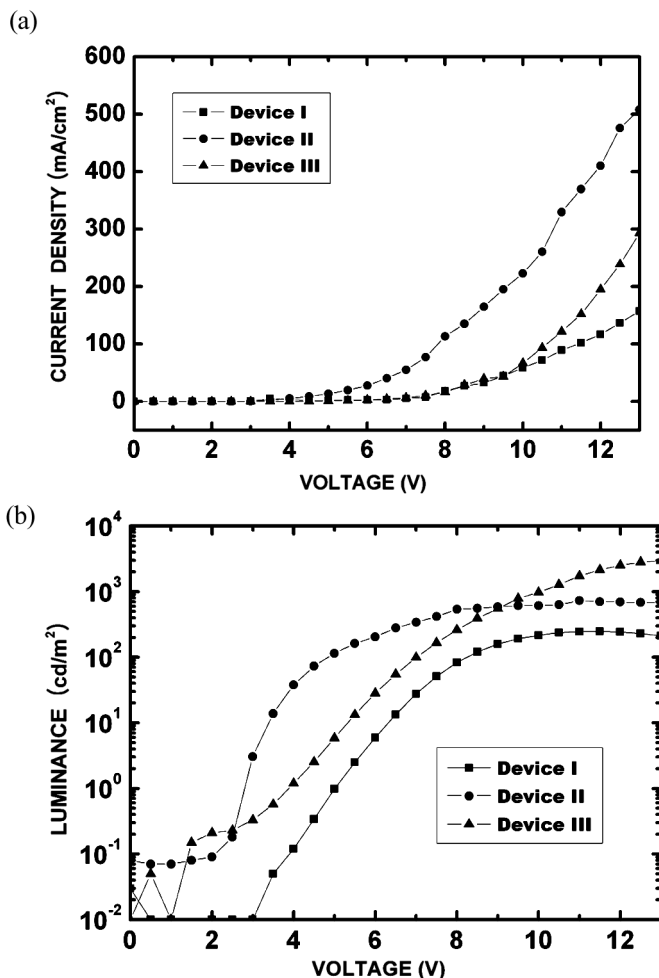
The current density-voltage and the luminance-voltage characteristics of devices I, II, and III are shown in Figures 2(a) and 2(b), respectively. The higher current density of device II in comparison with those of devices I and III is due to the insertion of the Liq layer acting as an electron injection layer (EIL). The luminance of device III above 9 V is larger than those of devices I and II resulting from the achievement of a better balance between the number of electrons and holes. The turn-on voltages of devices I, II, and III at 10 cd/m<sup>2</sup> are 6.3, 3.4, and 5.3 V, respectively.

Figure 3 shows  $\omega Z''-Z'$  characteristics and linear fitted lines for devices I, II, and III at (a) 3, (b) 5, and (c) 7 V. The  $\omega$ ,  $Z'$ , and  $Z''$  represent the angular frequency, the real and the imaginary parts of impedance, respectively. The frequency dependent impedances are converted into the  $\omega Z''-Z'$  plots. While the slopes of the fitting lines for devices I and II are one, those of device III are two, as shown in the insets of Figure 3(a) and 3(b), and in Figure 3(c). The slope of  $\omega Z''-Z'$  spaces corresponds to the inverse of relaxation time, which is described by the Debye model [20].

The relaxation time-voltage characteristics determined from the  $\omega Z''-Z'$  plots for devices I, II, III are shown in Figure 4. The relaxation time gradually decreases with increasing applied bias because the hopping conductivity is dependent on the hopping potential barrier. The relaxation time of hopping transition in the hopping conduction ( $\tau_{\text{hopping}}$ ) is given by [21–23]

$$\tau_{\text{hopping}} = \tau_0 \exp\left(\frac{\Delta E - E}{kT}\right), \quad (1)$$

where  $\tau_0$  is the hopping relaxation time at no potential barrier,  $\Delta E$  is the potential barrier,  $E$  is the applied electric field,  $k$  is the Boltzmann constant, and  $T$  is the absolute temperature, respectively. The relaxation time decreases with increasing electric field, as shown in Eq. (1). Therefore, the hopping conductivity increases with increasing electric field, and the dipoles formed between molecules are easy to be released by hopping charges. Because the transport carriers get larger



**FIGURE 2** (a) Current density-voltage and (b) luminance intensity-voltage characteristics for devices I, II, and III. Filled rectangles, filled circles, and filled triangles represent the OLEDs of devices I, II, and III, respectively.

activation energy for the hopping transition with an increase in the applied voltage, the relaxation time decreases. The relaxation time curve ( $\tau_1$ ) for device I is attributed to variation of relaxation time of dipole formed in Alq<sub>3</sub> molecules, and the shift of relaxation time ( $\tau_2$ ) for device II is related to the improvement of electron injection. The inserted Liq EIL in device II improves electron injection from the cathode electrode to the Alq<sub>3</sub> layer, resulting in the decrease of the  $\tau_2$

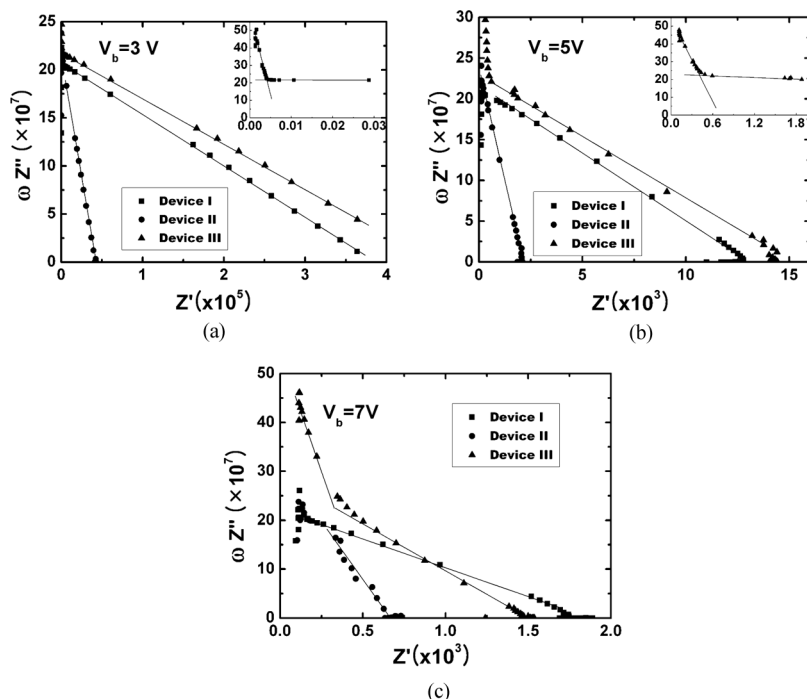


**FIGURE 3**  $\omega Z''$ - $Z'$  characteristics and linear fitted lines for devices I, II, and III at (a) 3, (b) 5, and (c) 7 V. The  $\omega$ ,  $Z'$ , and  $Z''$  represent the angular frequency, the real and the imaginary parts of impedance, respectively. Filled rectangles, filled circles, and filled triangles represent the OLEDs of devices I, II, and III, respectively.

due to an increase of the hopping electrons in the  $\text{Alq}_3$  layer. The shorter ( $\tau_{3,1}$ ) and longer ( $\tau_{3,2}$ ) relaxation times for device III correspond to the relaxation times of NPB and  $\text{Alq}_3$  layers, respectively. The variation of the  $\tau_{3,2}$  with increasing applied voltage is significantly different from those of  $\tau_1$ . The difference between  $\tau_{3,2}$  and  $\tau_1$  might be originated from the relaxation of dipoles due to the radiative recombination of electrons and holes. The dipoles are formed in an organic layer by applying the external electric field, and the number of dipoles decrease as the frequency increases. If the radiative recombination probability of dipoles were larger, the relaxation times become shorter. These reductions of relaxation times increase as the luminance increases. The variation of the differences between  $\tau_{3,2}$  and  $\tau_1$  are confirmed in Figure 4.



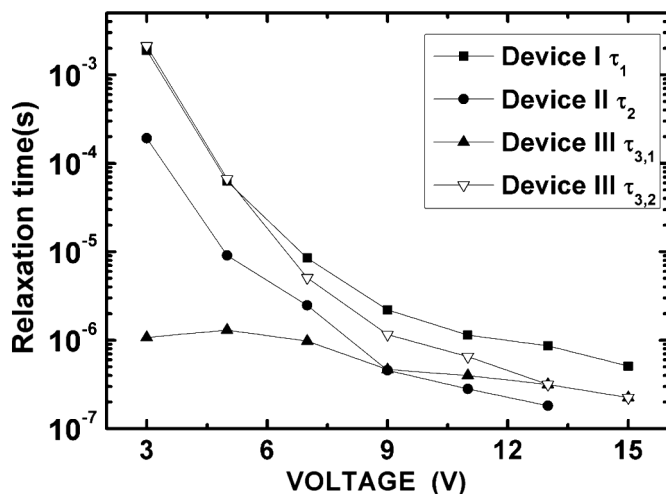


**FIGURE 4** Relaxation time-voltage characteristics for devices I, II, and III. Filled rectangles, filled circles, and filled triangles represent the OLEDs of devices I, II, and III, respectively, and empty triangles indicate the OLEDs of device III.

Figure 5 shows the experimental and theoretical Cole-Cole plots using a single-layer or a double-layer circuit model for devices I, II and III. The equivalent circuit models were designed using the relaxation times of dipoles for OLEDs at various voltages, as determined from the impedances as functions of the frequencies. The fitted lines of device I and II are calculated by the single layer model and that of device III is calculated by the double layer model, as shown in Figure 1(b). A slight deviation between the Cole-Cole plot data and the fitted lines in low frequency range might be attributed to the existence of other relaxation mechanisms [22–24]. The difference between the experimental and the theoretical results becomes large with increasing luminous intensity, and this behavior leads to a deviation from the Debye relaxation process. While the  $R_s$ ,  $C_p$  for devices I, II, and III are nearly constant values approximately  $100 \Omega$  and  $4.5 \times 10^{-9} \text{ F}$ , regardless of the variation of the applied voltage, respectively, the  $R_p$  decreases with increasing applied voltage.

#### IV. SUMMARY AND CONCLUSIONS

The frequency dependent impedances of single and double layer OLEDs at several applied biases were investigated. The relaxation

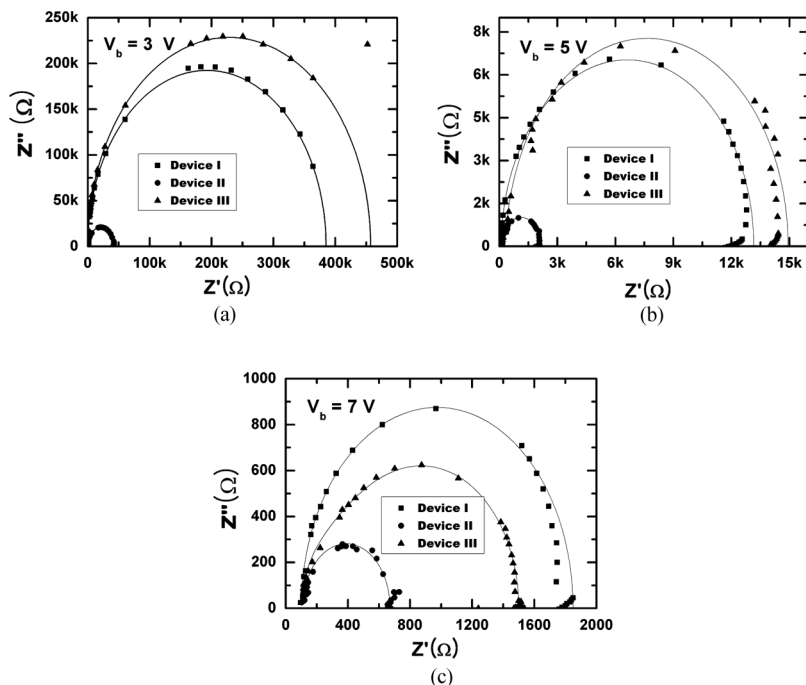


**FIGURE 5** Cole-Cole plots and the theoretical fitting data determined from the equivalent circuits using a single or a double layer model at (a) 3, (b) 5, and (c) 7 V. Filled rectangles, filled circles, and filled triangles represent the OLEDs of devices I, II, and III, respectively.

times of the OLEDs were determined from the frequency dependent impedances, and the equivalent circuits were designed on the basis of the relaxation time. The simulated Cole-Cole plots calculated from the equivalent circuits were in reasonable agreements with the experimental results. These equivalent circuit models for OLEDs with a single layer or a double layer can help designing equivalent circuit models of multilayer OLEDs.

## REFERENCES

- [1] Baldo, M. A., O'Brien, D. F., You, Y., Shoustikov, A., Sibley, S., Thompson, M. E., & Forrest, S. R. (1998). *Nature*, 395, 151.
- [2] Chuen, C. H. & Tao, Y. T. (2002). *Appl. Phys. Lett.*, 81, 4499.
- [3] Young, R. H., Tang, C. W., & Marchetti, A. P. (2002). *Appl. Phys. Lett.*, 80, 874.
- [4] Lewis, J., Grego, S., Chalamala, B., Vick, E., & Temple, D. (2004). *Appl. Phys. Lett.*, 85, 3450.

- [5] Kanno, H., Sun, Y., & Forrest, S. R. (2005). *Appl. Phys. Lett.*, 86, 263502.
- [6] Yan Shao & Yang Yang (2005). *Appl. Phys. Lett.*, 86, 073510.
- [7] Hagen, J. A., Li, W., Steckl, A. J., & Grote, J. G. (2006). *Appl. Phys. Lett.*, 88, 171109.
- [8] Campbell, A. J., Bradley, D. D. C., Laubender, J., & Sokolowski, M. (1999). *J. Appl. Phys.*, 86, 5004.
- [9] Berleb, S., Brütting, W., & Paasch, G. (2001). *Synthetic Metals*, 122, 37.
- [10] Ono, R., Kiy, M., Biaggio, I., & Günter, P. (2001). *Mater. Scien. & Engin.*, B85, 144.
- [11] Kim, S. H., Lim, S. C., Lee, J. H., & Zyung, T. (2005). *Curr. Appl. Phys.*, 5, 35.
- [12] Campbell, I. H., Smith, D. L., & Ferraris, J. P. (1995). *Appl. Phys. Lett.*, 66, 3030.
- [13] Rhee, H. W., Chin, K. S., Oh, S. Y., & Choi, J. W. (2000). *Thin Solid Films*, 363, 236.
- [14] Brütting, W., Riel, H., Beierlein, T., & Riess, W. (2001). *J. Appl. Phys.*, 89, 1704.
- [15] Hulea, I. N., van der Scheer, R. F. J., Brom, Bea, H. B., Langeveld-Voss, M. W., van Dijken, A., & Brunner, K. (2003). *Appl. Phys. Lett.*, 83, 1246.
- [16] Shrotriya, V. & Yang, Y. (2005). *J. Appl. Phys.*, 97, 054504.
- [17] Petty, M. C., Pearson, C., Monkman, A. P., Casalini, R., Capaccioli, S., & Nagel, J. (2000). *Colloids. Surf. A: Physicochem. Eng. Aspects*, 171, 159.
- [18] Pingree, L. S. C., Scott, B. J., Russell, M. T., Marks, T. J., & Hersam, M. C. (2005). *Appl. Phys. Lett.*, 86, 073509.
- [19] Liu, D., Teng, F., Xu, Z., Yang, S., Quan, S., He, Q., Wang, Y., & Xu, X. (2006). *Solid. State. Commun.*, 137, 391.
- [20] Raju, G. G. (2003). *Dielectrics in Electric Field*, Marcel Dekker: New York.
- [21] Dyre, J. C. (1988). *J. Appl. Phys.*, 64, 2456.
- [22] Kao, K. C. (2004). *Dielectric Phenomena in Solid*. Elsevier Academic Press: California, Chapter 2, p. 41, Chapter 7, p. 381.
- [23] Kim, S. H., Choi, K. H., Lee, H. M., Hwang, D. H., Do, L. M., Chu, H. Y., & Zyung, T. (2000). *J. Appl. Phys.*, 87, 882.
- [24] Bak, G. W. & Jonscher, A. K. (1999). *J. Mater. Sci.*, 34, 5505.